Supporting Information for

DNA-Engineered Iron Single-Atom Nanozyme for mRNA-Guided Dual-Pathway Modulation in Enhanced Mild Photothermal Therapy

Zixuan Liu, ‡[a] Fanghua Zhang, ‡[a] Wendong Liu, [a] Zhe Hao, [a] Yuxin Wang, [a] Hongyan Zhang, [a] Ruizhong Zhang,* [a] Xiyan Li,* [b] and Libing Zhang* [a]

[a] *Tianjin Key Laboratory of Molecular Optoelectronic Sciences, Department of Chemistry, School of Science, Tianjin University, Tianjin, 300072, P. R. China.*
Email: zhangrz2019@tju.edu.cn; libing.zhang@tju.edu.cn

[b] *Institute of Photoelectronic Thin Film Devices and Technology, Solar Energy Conversion Center, Nankai University, Tianjin 300350, China.*
Email: xiyan.li@nankai.edu.cn

Materials and methods:

Chemical and materials. All DNA oligonucleotide sequences were purchased from Sangon Biotechnology Co. Ltd. (Shanghai, China) and listed in Table S2. Zinc nitrate hexahydrate (Zn $(NO_3)_2 \cdot 6H_2O$), Hemin (95%), 2-methylimidazole (MeIM), and H_2O_2 (30%) were obtained from Aladdin Industrial Corp. (Shanghai, China). 3,3',5,5'-tetramethylbenzidine (TMB), glutathione (GSH), and terephthalic acid (TA) were purchased from Sigma-Aldrich (St Louis, MO, USA). All the chemicals were used as received without further purification. Deoxyribonuclease I (DNase I), Dulbecco's modified eagle medium (DMEM, high glucose), 3-(4,5 Dimethylthiazole)-2,5-diphenyltetrazolium bromide (MTT), and 2-(4-amidinophenyl)-6-indolecarbamidine dihydrochloride (DAPI), and Trypsin were purchased from Sangon Biotech Co., Ltd. (Shanghai, China). Mitochondrial membrane potential assay kits with JC-1 and a Live/Dead Cell Staining Kit were obtained from Beyotime Biotechnology (Shanghai, China). HSP90 antibody was purchased from Bioss (Bioss, China).

Instrument. Transmission electron microscopy (TEM) images and elemental mappings were obtained using a JEM-2100F with an accelerating voltage of 200 kV. Scanning electron microscopy (SEM) images were captured on a TESCAN MIRA LMS (Czech). X-ray photoelectron spectroscopy (XPS) measurements were conducted on a Thermo Scientific K-Alpha. The crystal structure of the samples was analyzed by X-ray diffraction (XRD) with Cu Kα radiation (Rigaku SmartLab SE, Japan). Zeta potential was measured using a Zetasizer nano ZS90 (Malvern Panalytical). Ultraviolet-visible (UV-vis) absorption spectra were recorded on a UV-vis-NIR spectrophotometer (UV-3600 Plus, Shimadzu, Japan). Gel imaging was performed on a Tanon 5200 (Tanon, China) under UV irradiation (λ = 365 nm). Fluorescence analysis was carried out using an FS05 steady-state transient fluorescence spectrometer (Edinburgh, England), and cell viability assays were conducted on an Infinite E Plex (Tecan, Austria). Confocal laser scanning microscopy (CLSM) images were obtained using a Nikon A1R+ (Japan) confocal microscope.

Synthesis of Hemin@ZIF-8. The precursor hemin@ZIF-8 was synthesized through a straightforward chemical precipitation method using 2-methylimidazole (MeIM), $Zn(NO_3)_2 \cdot 6H_2O$, and hemin as starting materials in a methanol solvent. In a typical procedure, MeIM (2.36 g) and hemin (55 mg) were dissolved in 40 mL of methanol solution. $Zn(NO_3)_2 \cdot 6H_2O$ (1.07 g) was dissolved in another 40 mL of methanol. The $Zn(NO_3)_2 \cdot 6H_2O$ solution was then poured into the MeIM-hemin solution and stirred at room temperature for 24 hours. The resulting product was collected by centrifugation, washed thoroughly with methanol three times, and dried overnight in a vacuum oven at 70 °C.

Detection of hydroxyl radical (•OH). Fe-N-C@DNA (60 μg mL^{-1}) or Fe-N-C (60 μg mL^{-1}) were added to a solution of HAc-NaAc (0.02 M, pH 4.0) containing 0.4 mM H_2O_2

and 200 μM DMPO for EPR testing to measure •OH generation. •OH was also investigated using terephthalic acid (TA). The solutions including TA, TA + H_2O_2, or TA + H_2O_2 + Fe-N-C@DNA with different concentrations (0, 0.2, 0.4, 0.6, 0.8, 1 μM) were reacted for 3 h at room temperature and then centrifuged.

GSH Depletion. GSH depletion was assessed using Ellman's assay. 100 μL GSH (10 mM) was added to a mixture of 25 μL Fe-N-C@DNA with different concentrations (10, 30, 50 μg mL^{-1}) and 875 μL PBS (0.1 M, pH 7.4). Next, the mixture was centrifuged (13000 rpm, 3 minutes) to obtain the supernatant. 100 μL of supernatant was then added to the solution containing 25 μL of DTNB (1.5 mg mL^{-1}) in 875 μL PBS (0.1 M, pH 7.4). The absorbance was measured at 410 nm after incubation at room temperature for different times (0, 15, 30, 60, 90, 120 min).

Photothermal Conversion Efficiency. The photothermal conversion efficiency was calculated according to the previously described method, and the formula is as follows:

$$\eta = \frac{hS(Tmax - Tsurr) - Q_0}{I(1 - 10^{-A_{808}})\tau s} \quad (1)$$

$$\tau s = \frac{mdCd}{hS} \quad (2)$$

$$Q0 = hS(Tmax,water - Tsurr) \quad (3)$$

$$t = -\tau_s \ln(\vartheta) = -\tau_s \ln(T - Tsurr)/(Tmax - Tsurr) \quad (4)$$

η is the photothermal conversion efficiency. h is the system heat conversion efficiency, S is the surface area of the container, and the value of hS can be determined according to formula (2). T_{max} is the stable maximum temperature of the sample and T_{surr} is the environmental temperature. $T_{max,water}$ represents the stable maximum temperature of the water. Q_0 is the change in heat when the reagent is blank, as calculated using formula (3). I is the laser power and A_{808} is the absorbance value of the sample at 808 nm. m_d is the mass of the solution and C_d is the specific heat capacity of the solution. ϑ is the driving force temperature. The linear relationship between time and $-\ln\vartheta$ is calculated for the rise and fall curves of a single cycle. τ_s is the time constant of the system and can be obtained by linearly fitting the negative value of the natural logarithm of the cooling time to the thermal drive constant, which is determined from the formula (4).

DNA Loading Capacity on Fe-N-C@DNA. 5 μL of FAM-labeled 1 μM DNA was incubated with different concentrations of Fe-N-C (0, 20, 30, 40, 50, 60, 70, 80, 90 μg mL^{-1}, 95 μL) at 25 ℃ for 15 min. After centrifugation at 14000 rpm for 7 min, Fe-N-C

was completely separated from DNA. The supernatant was collected and its fluorescence intensity was measured using a fluorescence spectrophotometer.

Optimal incubation time for Fe-N-C@DNA. 5 μL of FAM-labeled 1 μM DNA and 95 μL 60 μg mL^{-1} Fe-N-C were incubated for different times (0, 5, 10, 15, 30, 45, 60, 75, 90, 120 min) at 25 ℃. The mixtures were centrifuged at 14000 rpm for 7 min, and then the fluorescence of supernatants was monitored.

Optimal incubation time of the Fe-N-C@DNA to HSP90 mRNA. Fe-N-C@DNA and HSP 90 mRNA were co-incubated at 37 ℃ for different times (0, 30, 60, 90, 150, 180 min) for hybridization. After centrifugation at 14000 rpm for 7 min, the fluorescence signal of the supernatant was detected.

Specificity Response Experiment. The Fe-N-C@DNA nanomaterial was combined with the interfering substance (HSP90-M1, HSP90-M2, c-myc, piRNA, MCM2) and the target HSP90 mRNA, respectively. After incubation at 37 ℃ for 90 min, the fluorescence signal of the supernatant was collected after centrifugation.

Stability Experiment of the Fe-N-C@DNA Nanomaterial. DNA (50 nM) was used as the control group, while Fe-N-C@DNA nanomaterial (50 nM) was incubated in two experimental groups: (1) Fe-N-C@DNA alone and (2) Fe-N-C@DNA with DNase I (5 U L^{-1}) at 37 °C. The fluorescence intensity of the supernatant was monitored at different incubation times (0, 15, 30, 45, 60 min).

Cell viability assay. MCF-7 and MCF-10A cells were seeded into 96-well plates with 1×10^4 cells/well and incubated at 37 ℃ overnight. After adding fresh media with varying concentrations of Fe-N-C@DNA nanomaterials (0, 5, 15, 30, 45, 60, 75, 90, 120 μg mL^{-1}), cell viability was measured by the MTT method after 24 hours.

To evaluate the therapeutic effect, cells were cultured in media containing different concentrations of Fe-N-C and Fe-N-C@DNA (0, 5, 15, 30, 45, 60, 75, 90 μg mL^{-1}) and irradiated with or without near-infrared (NIR) light (808 nm, 0.5 W cm^{-2}, 5 min) 4 hours after the addition of the materials. After 24 hours of incubation, cell viability was assessed using the MTT method.

Additionally, live/dead cell analysis was performed to observe the therapeutic effect. MCF-7 cells were seeded in 6-well plates at a density of 1.5×10^5 cells per well and incubated for 24 hours. The cells were treated with 60 μg mL^{-1} of Fe-N-C or Fe-N-C@DNA, with a PBS group serving as the control. After 4 hours of incubation, the cells were either exposed or not exposed to NIR irradiation (808 nm, 0.5 W cm^{-2}, 5 min), followed by a further 24 hours of incubation. The cells were then washed twice with PBS, stained with calcein AM and propidium iodide (PI) for 30 minutes at 37 ℃ in the dark, and examined under a fluorescence microscope to evaluate cell viability.

Intracellular Uptake of the Fe-N-C@DNA Nanomaterial. MCF-7 cells were seeded in confocal dishes at 37 ℃ overnight, with 100 μg mL^{-1} Fe-N-C@DNA nanomaterial

added, and then incubated for different times (1, 2, 4, 6 h). After washing with PBS three times, the cells were fixed with the 4% paraformaldehyde for 20 min and then stained with DAPI (2 μg mL^{-1}) for 15 min. The cells were washed three times with PBS and observed by confocal microscopy.

Analysis of mitochondrial membrane potential. MCF-7 cells (1×10^5 cells) were seeded into confocal dishes, and the nanomaterials were added by repeating the above procedure. Then JC-1 was added and incubated at 37 ℃ without light for 30 min. After washing with PBS twice, the treated cells were observed by a confocal laser scanning microscope.

Western blot assay. MCF-7 cells were seeded in 6-well plates and cultured overnight at 37 ℃. For the laser irradiation group, after incubating the cells with culture medium containing Fe-N-C (60 μg mL^{-1}) or Fe-N-C@DNA (60 μg mL^{-1}) for 4 h, the cells were exposed to 808 nm laser irradiation (0.5 W cm^{-2}) for 5 min and then further cultured for 20 h. For the non-laser irradiation group, the cells were cultured for 24 h at 37 ℃ with medium containing PBS, Fe-N-C (60 μg mL^{-1}), or Fe-N-C (60 μg mL^{-1}) + NAC. The cells were lysed on ice with RIPA cracking buffer for 15 min. After centrifugation at 10000 rpm for 10 min (4 ℃), the supernatant was collected and the protein concentration was quantified using a BCA kit. The protein samples were separated by sodium dodecyl sulfate-polyacrylamide gel electrophoresis (SDS-PAGE) and transferred onto a polyvinylidene fluoride (PVDF) membrane. PVDF membrane was treated with HSP90 primary antibody (1:1000) and horseradish peroxidase conjugate secondary antibody, and β-actin was used as the protein loading control. Finally, the membrane was visualized by incubation with the chemiluminescent substrate.

Biodistribution *in vivo*. MCF-7 tumor-bearing mice were intravenously injected with Fe-N-C@DNA (2 mg mL^{-1}). Following the injection, *in vivo* fluorescence imaging was performed at 0, 2, 12, and 24 h. The mice were euthanized 24 h post-injection, and major organs (heart, liver, spleen, lung, kidney) along with tumors were harvested for in vitro fluorescence imaging. For photothermal imaging, the mice were divided into two groups, with three mice per group: Group 1 received PBS, while Group 2 received Fe-N-C@DNA (2 mg mL^{-1}). 12 h after intravenous injection, tumors in the mice were irradiated with an 808 nm near-infrared laser (0.5 W cm^{-2}, 5 min), and the temperature change in the tumor tissue was monitored using a near-infrared camera.

Supporting tables and figures

Table S1 Comparison of the apparent Michaelis-Menten constant (K_m) and maximum reaction rate (V_{max}) of the catalytic reactions.

Catalyst	**Substrate**	K_m **(mM)**	V_{max} **(10^{-6} M/s)**
Fe-N-C	TMB	1.36571	0.26073
	H_2O_2	3.16723	0.25127
Fe-N-C@DNA	TMB	0.11488	7.54
	H_2O_2	2.972	7.54

Table S2 The photothermal conversion efficiency for the previously reported ZIF-8 based Fe single-atom nanomaterials and the as-prepared Fe-N-C@DNA.

Nanozymes	PCE (η)	Ref.
PSAF	19.21%	[1]
SAF NCs	19.37%	[2]
(Fe, Pt) SA-N-C	36.8%	[3]
Fe-N-C@DNA	47.4%	This work

Table S3 Sequences of synthesized DNA and RNA.

Name	**Sequences (5'-3')**
DNA1	AAAAAAAAAAAAAAACTGTAATCCGGGAGCACACG
DNA2	TCTGTGCCTACGTGTGCTCCCGG
HAP90 mRNA	GGAGCACACGUAGGCACAGA
c-myc	CCUCAACGUUAGCUUCACCAA
MCM2	UUCCAUGCCAUCTCCAAUGAGCUCC
piRNA	CGUGAGAGCGCC
M1	GGAGCACACGCAGGCACAGA
M2	GGAGCAUACGUAGACACAGA

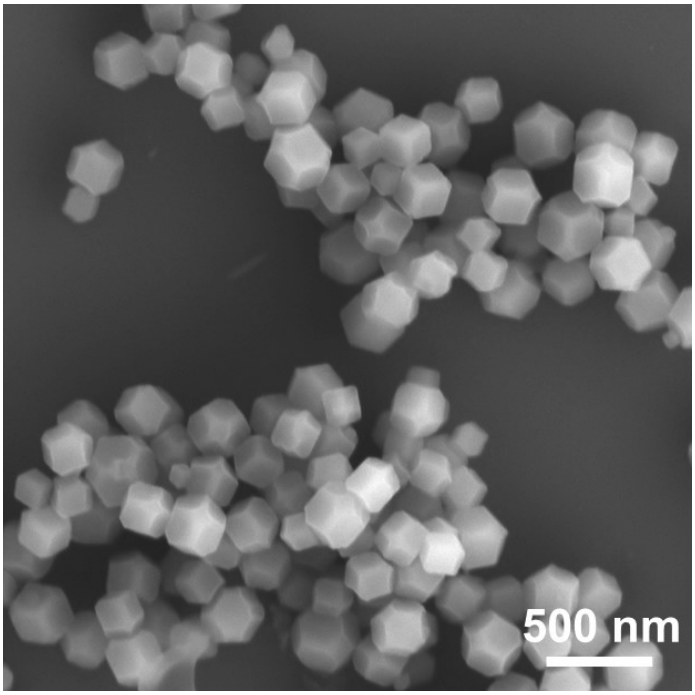

Fig. S1 SEM image of Hemin@ZIF-8 precursors.

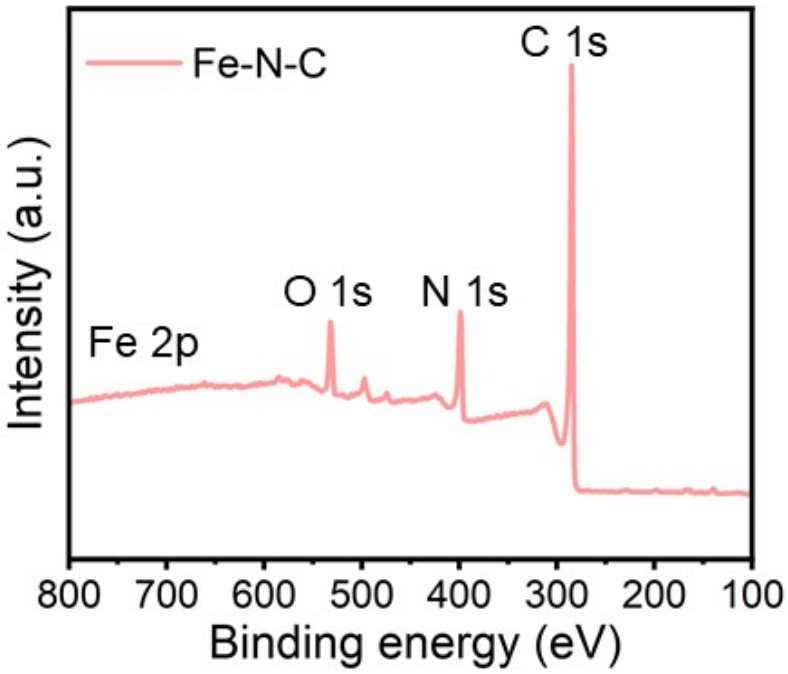

Fig. S2 XPS survey spectrum of Fe-N-C.

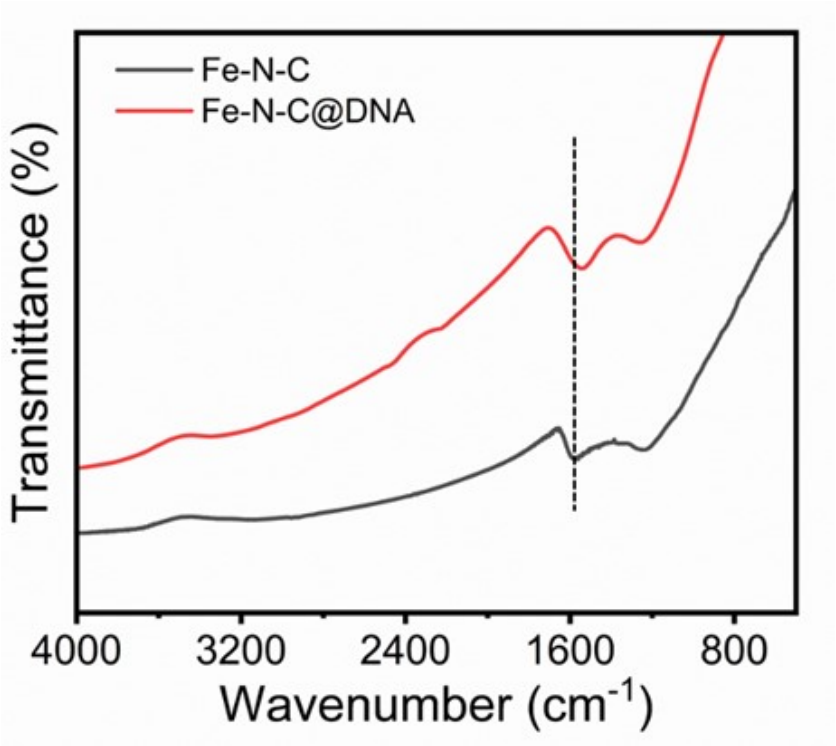

Fig. S3 FTIR spectra of Fe-N-C and Fe-N-C@DNA.

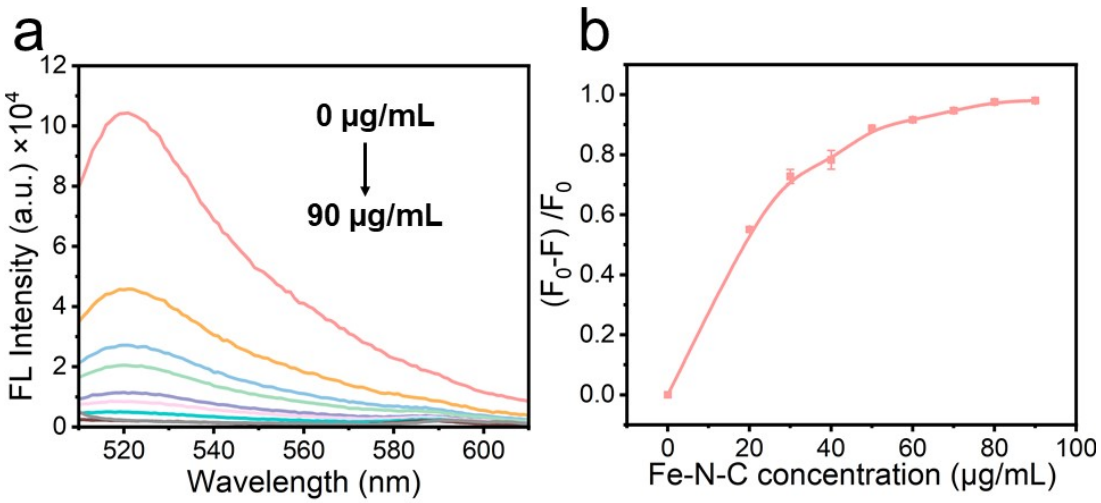

Fig. S4 (a) Fluorescence spectra and (b) fluorescence intensity of centrifugation supernatant of 50 nM FAM-labeled DNA incubated with different concentrations of Fe-N-C.

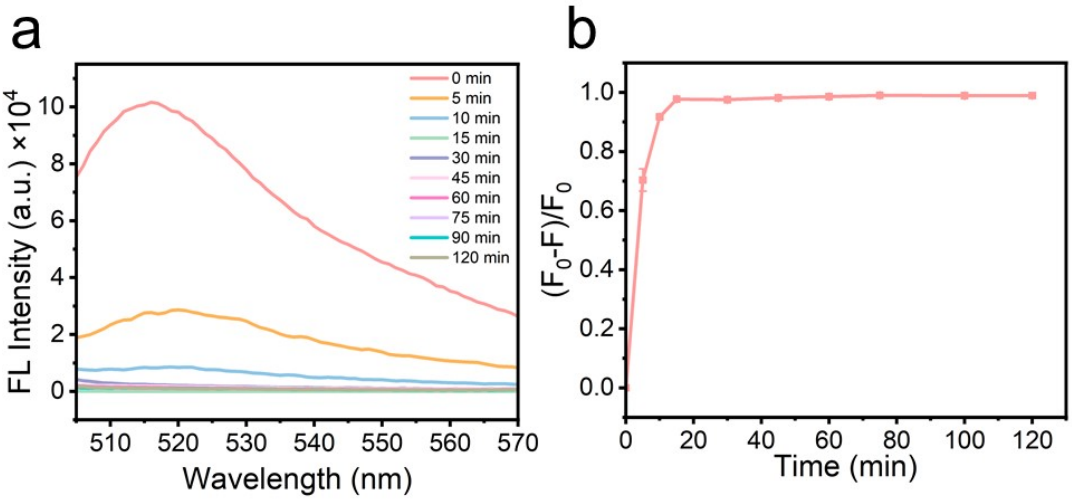

Fig. S5 (a) Fluorescence spectra and (b) fluorescence intensity of centrifugation supernatant of 50 nM FAM-labeled DNA incubated with Fe-N-C (60 μg mL^{-1}) at different incubation times.

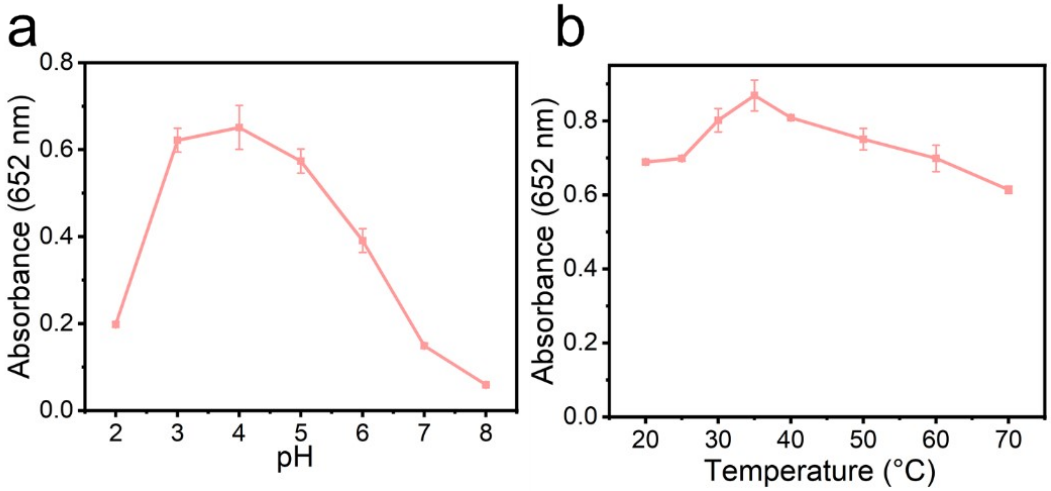

Fig. S6 The variation in absorbance of Fe-N-C@DNA as a function of (a) pH and (b) temperature was measured, with absorbance recorded at 652 nm.

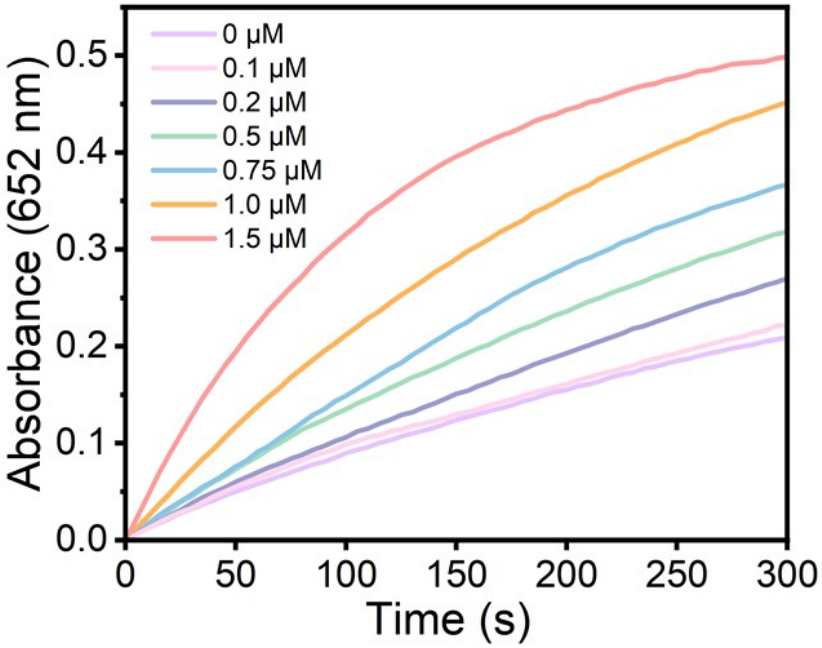

Fig. S7 The POD-like activity of the Fe-N-C@DNA at different DNA concentrations by monitoring the absorption of TMB at 652 nm.

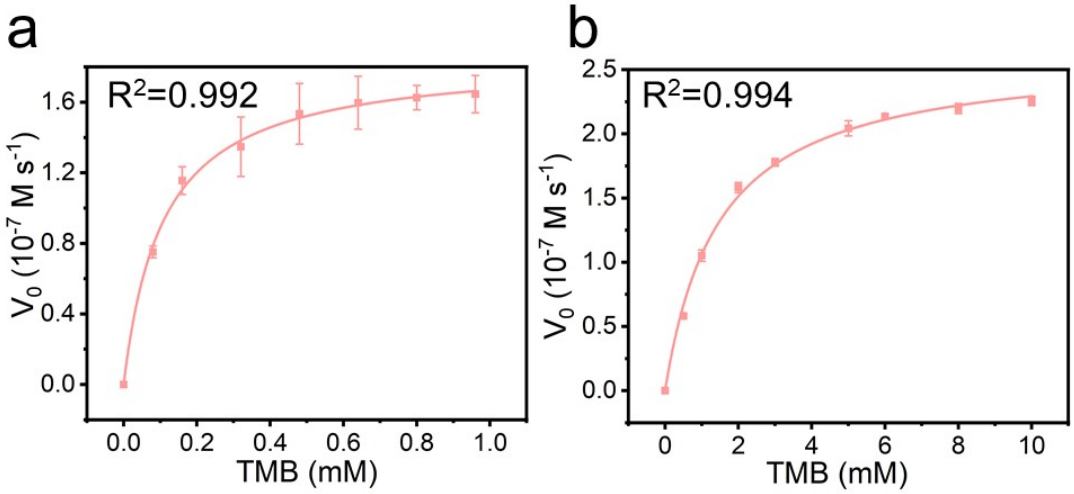

Fig. S8 Michaelis-Menten kinetics of (a) Fe- N-C and (b) Fe-N-C@DNA for TMB.

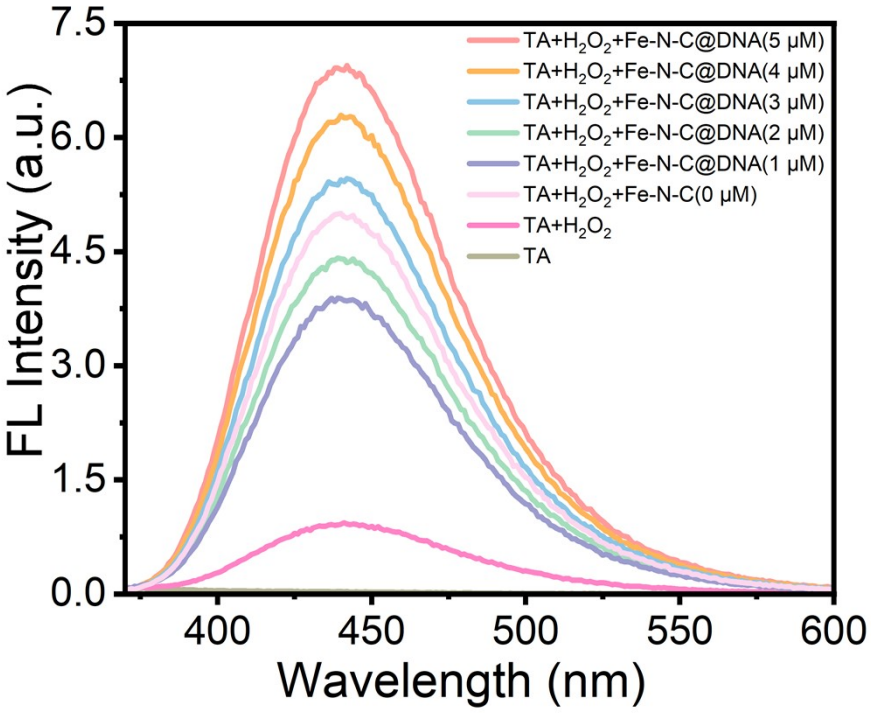

Fig. S9 Fluorescent spectra of TA in different reaction systems.

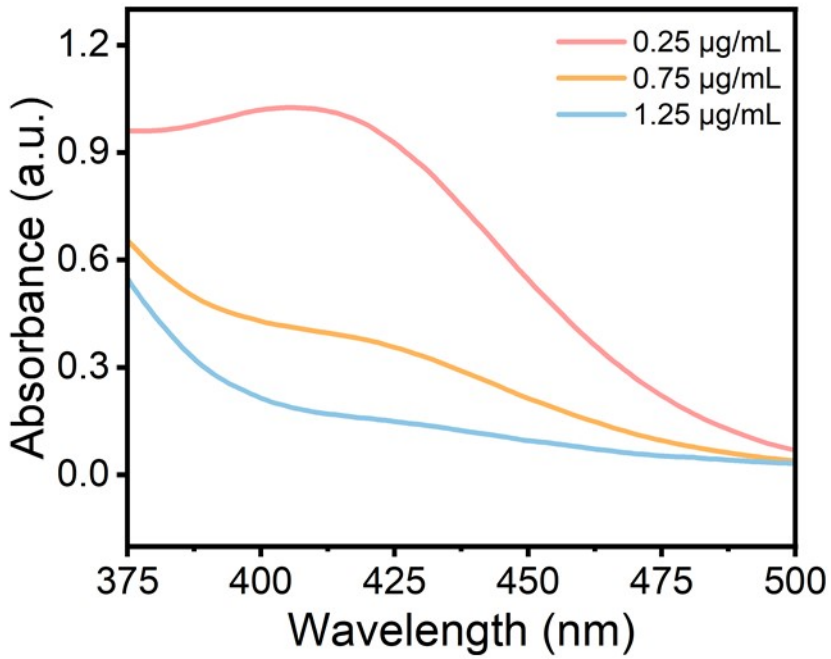

Fig. S10 GSH depletion by different concentrations Fe-N-C@DNA characterized by the absorbance of DTNB.

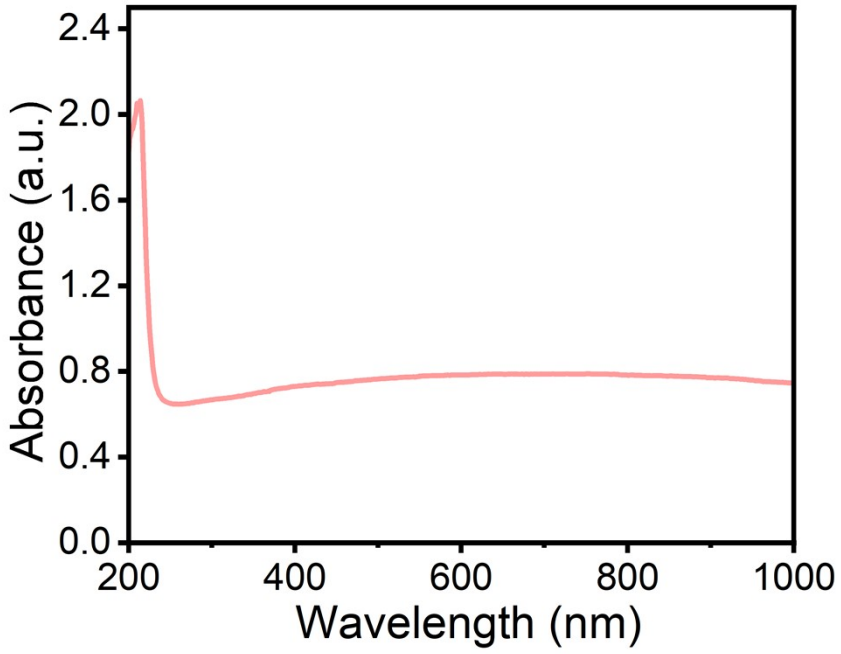

Fig. S11 Vis/NIR absorption spectrum of Fe-N-C.

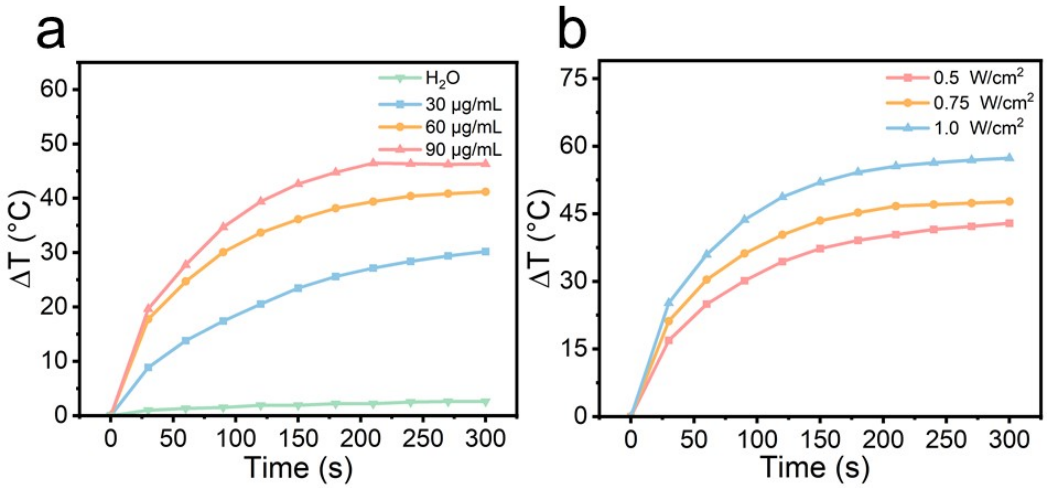

Fig. S12 (a) Temperature variation curves of Fe-N-C@DNA aqueous solution with different concentrations (0, 30, 60, and 90 μg mL^{-1}) under 808 nm laser. **(**b) Temperature variation curves of Fe-N-C@DNA aqueous solution (60 μg mL^{-1}) at different laser power intensities.

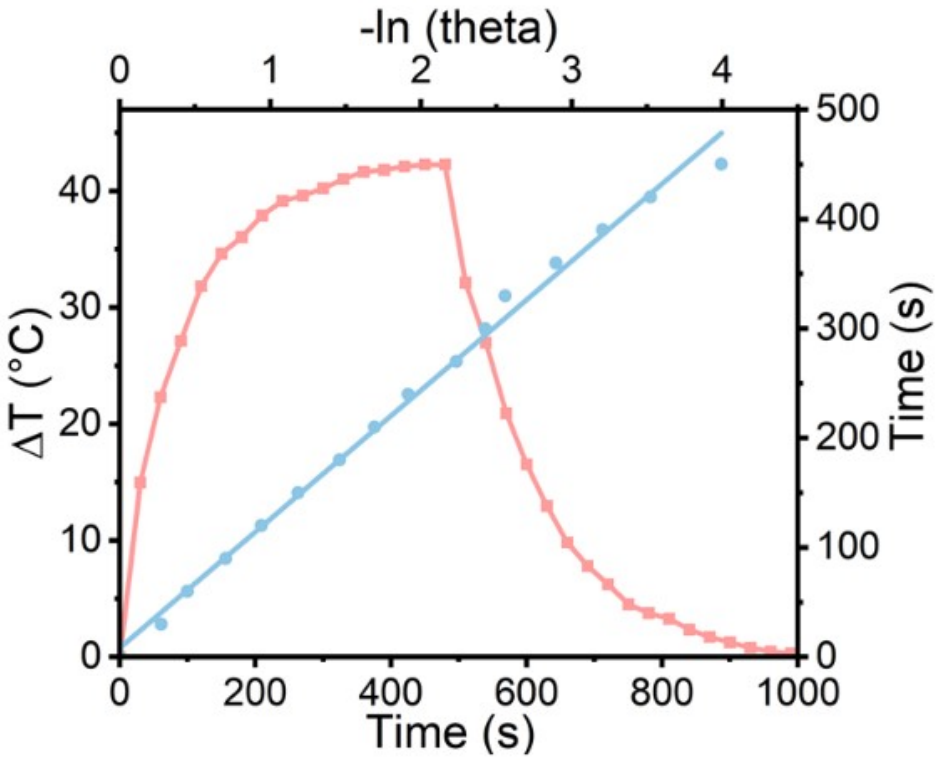

Fig. S13 Heating and cooling curve of Fe-N-C@DNA (60 μg mL^{-1}) under the NIR laser (808 nm, 0.5 W cm^{-2}) and photothermal conversion efficiency.

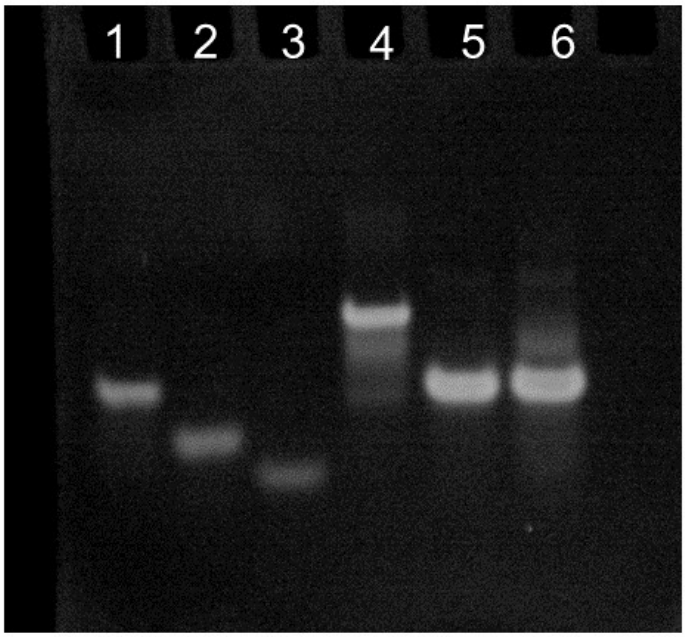

Fig. S14 Gel electrophoresis images of the nanomaterial for HSP90 mRNA detection (lane 1: DNA1, lane 2: DNA2, lane 3: HSP90 mRNA, lane 4: DNA1+DNA2, lane 5: DNA2+HSP90 mRNA, lane 6: DNA1+DNA2+HSP90 mRNA).

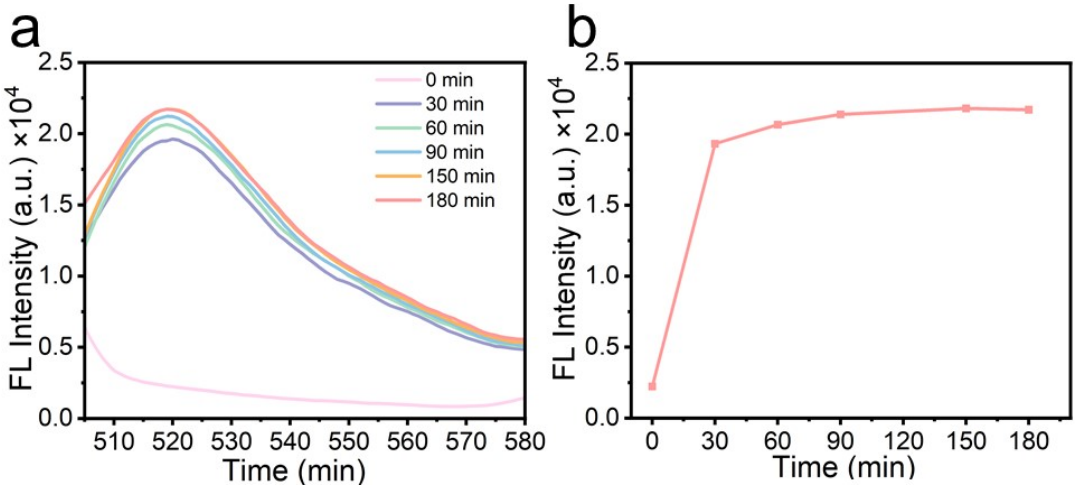

Fig. S15 (a) Fluorescence spectra and (b) fluorescence intensity of centrifugation supernatant of HSP90 mRNA (50 nM) incubated with Fe-N-C@DNA at different incubation time.

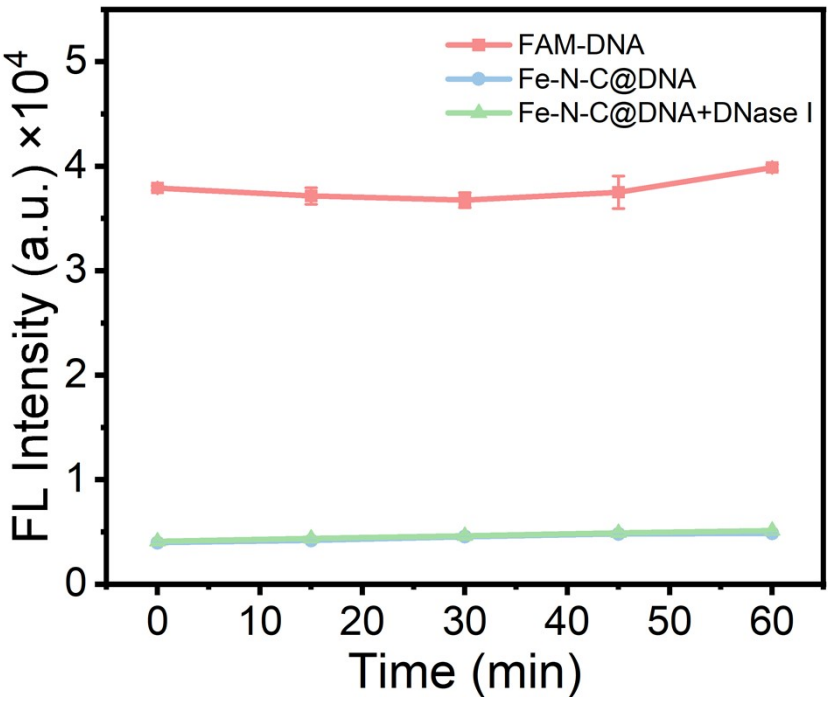

Fig. S16 Fluorescence intensities of the FAM-DNA, Fe-N-C@DNA and the Fe-N-C@DNA treated with 0.5 U mL^{-1} DNase I for diverse periods.

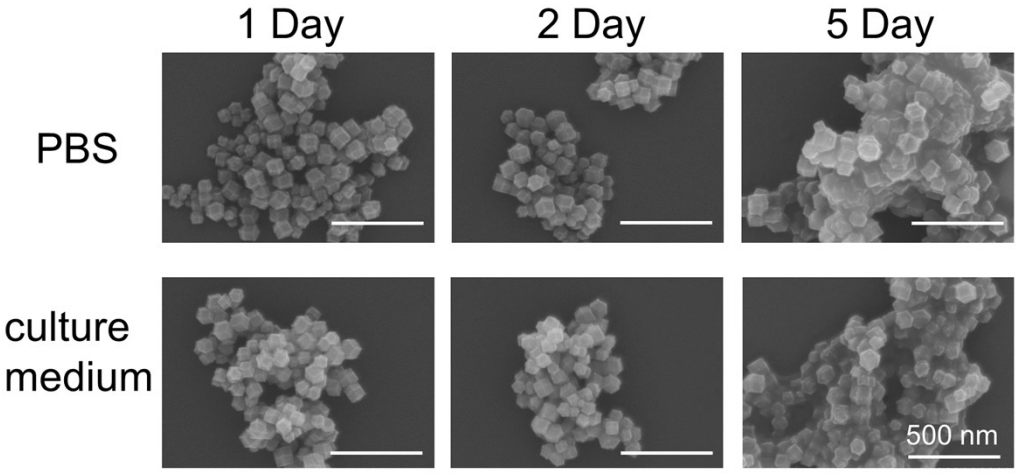

Fig. S17 SEM images of Fe-N-C@DNA after incubation in PBS and culture medium for different durations.

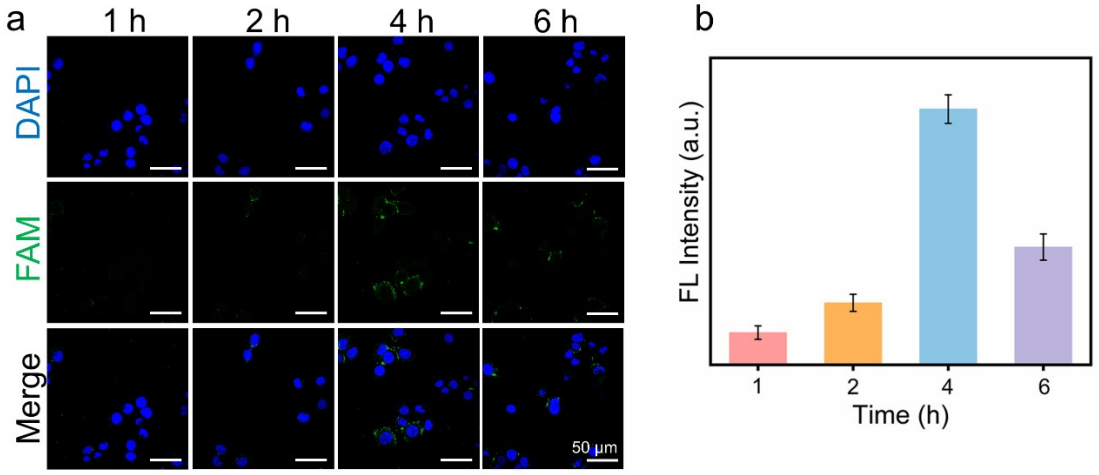

Fig. S18 (a) The CLSM images and (b) the fluorescence intensity of MCF-7 cells after incubating with the Fe-N-C@DNA nanomaterials for different times (1, 2, 4, 6 h).

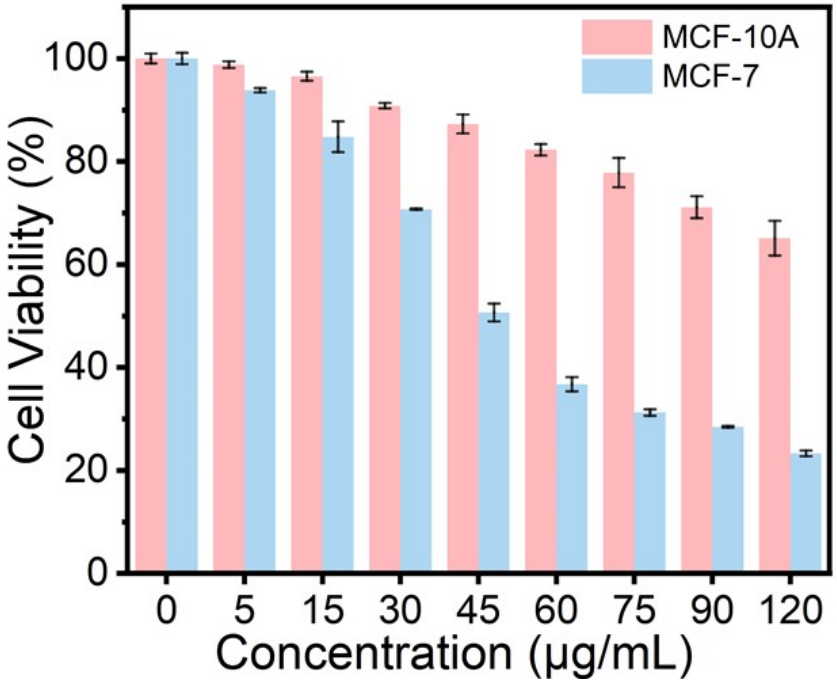

Fig. S19 Cytotoxicity assessment of different concentrations of Fe-N-C@DNA tested on MCF-7 and MCF-10A cells.

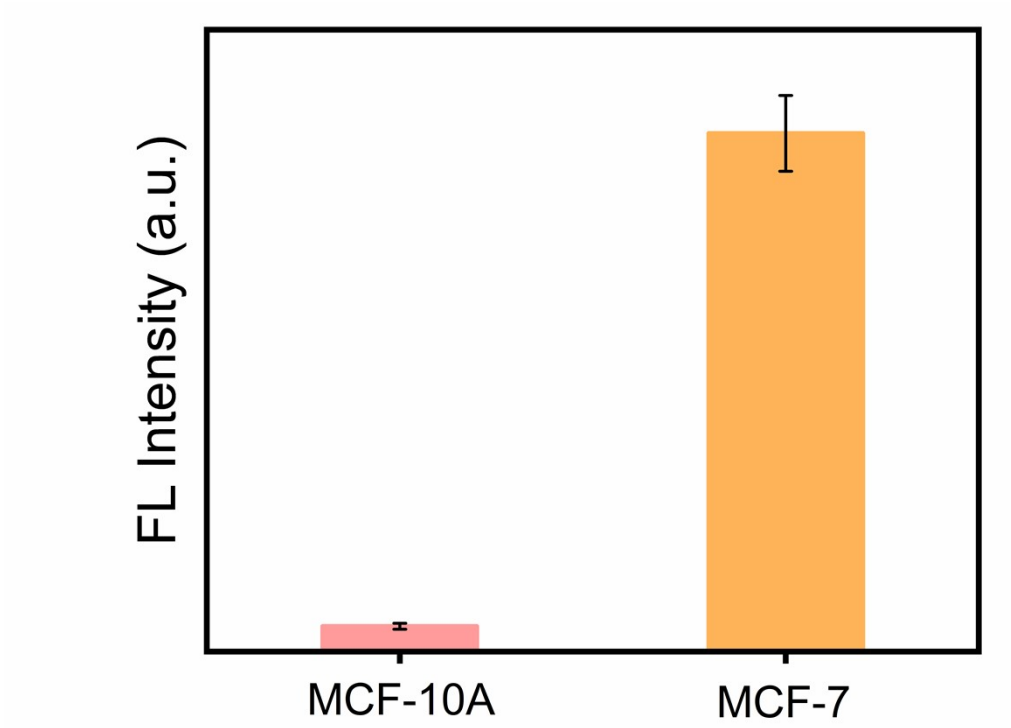

Fig. S20 The fluorescence intensities of imaging MCF-10A and MCF-7 cells.

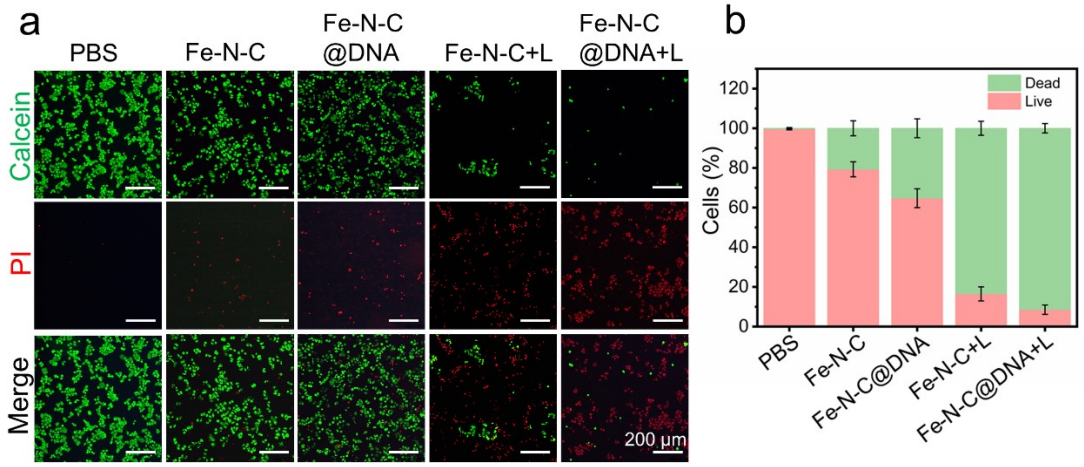

Fig. S21 (a) Fluorescence images and (b) the fluorescence intensity of Calcein-AM/PI staining of MCF-7 cells after different treatments.

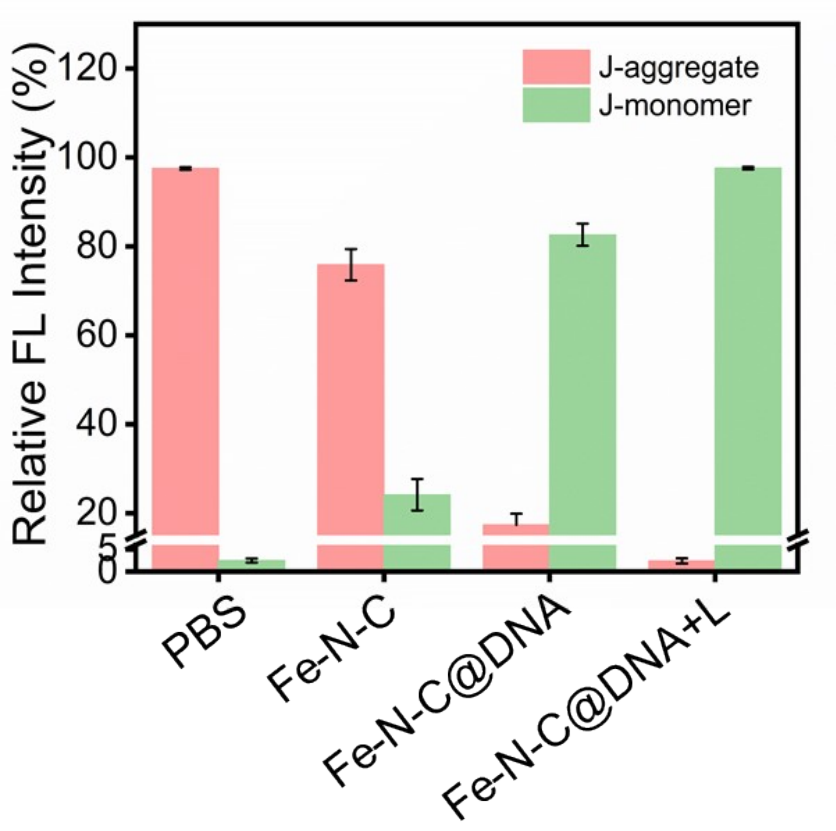

Fig. S22 The fluorescence intensity of mitochondrial membrane potential in MCF-7 cells under different conditions.

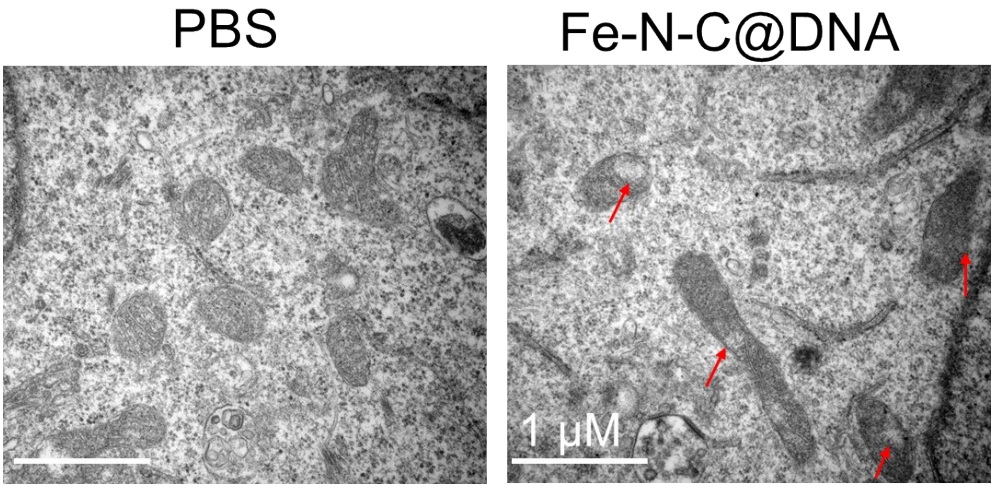

Fig. S23 MCF-7 cell morphology after the incubation with PBS and Fe-N-C@DNA by Bio-TEM.

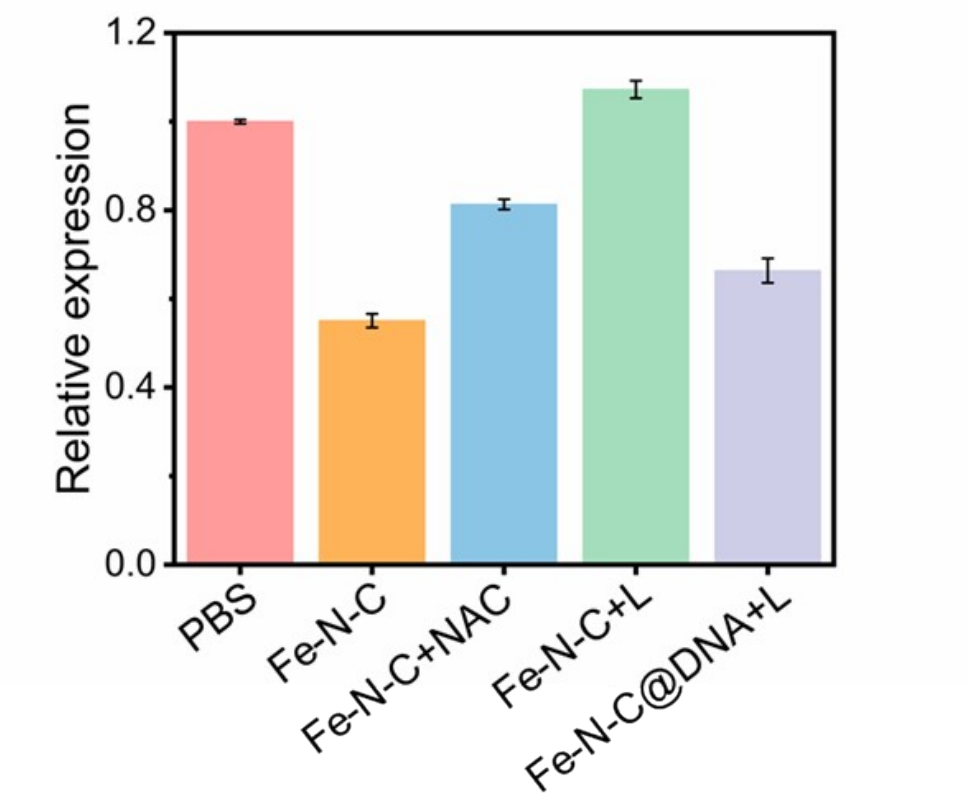

Fig. S24 Gray analysis of western blotting.

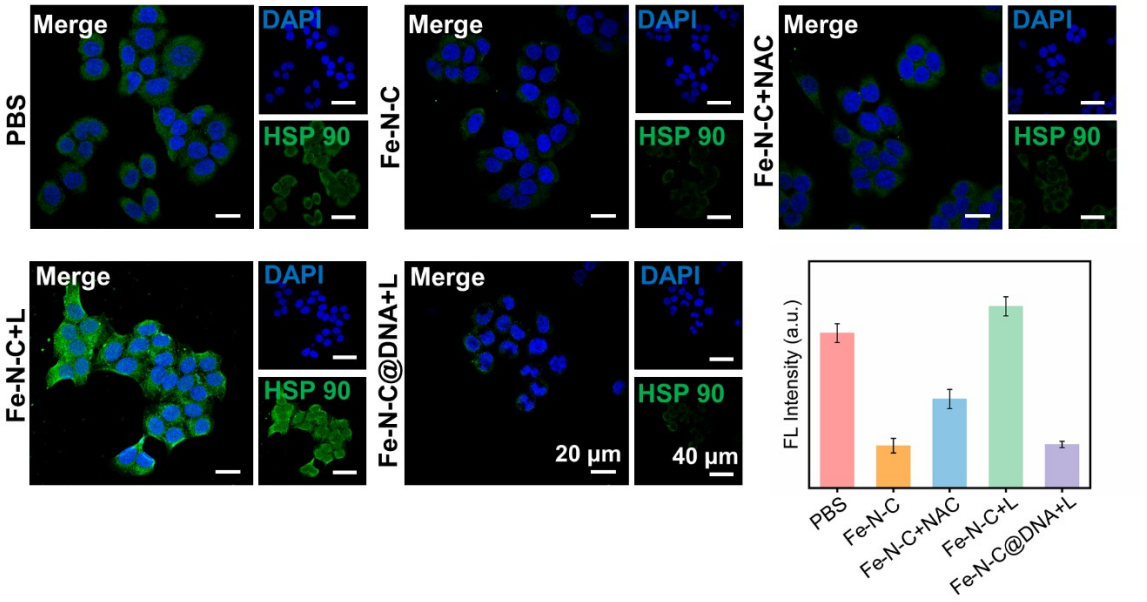

Fig. S25 CLSM-based immunofluorescence detection of HSP90 expression in MCF-7 cells treated with different recipes.

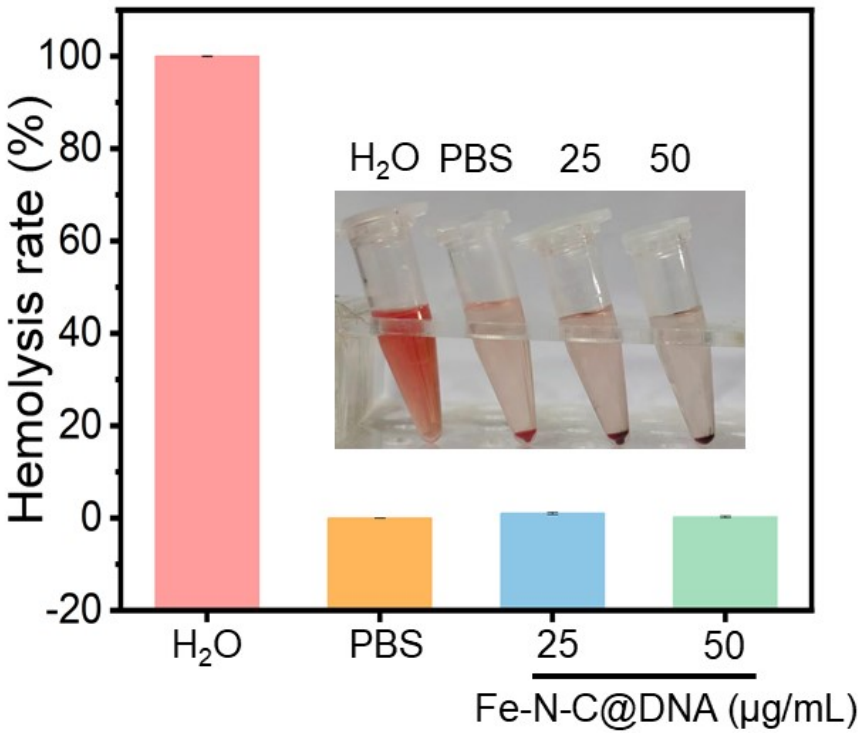

Fig. S26 Hemolysis rate of H_2O, PBS, and Fe-N-C@DNA at different concentrations.

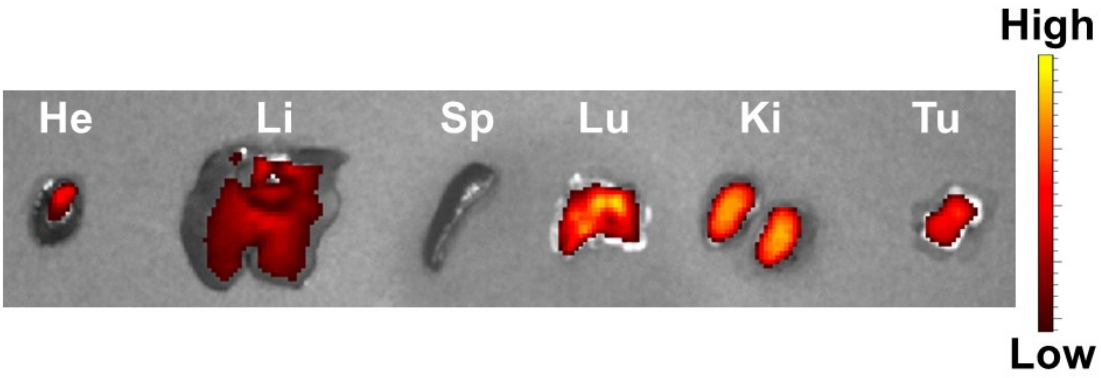

Fig. S27 Fluorescence images of major organs and tumors after injection of Fe-N-C@DNA after 24 h.

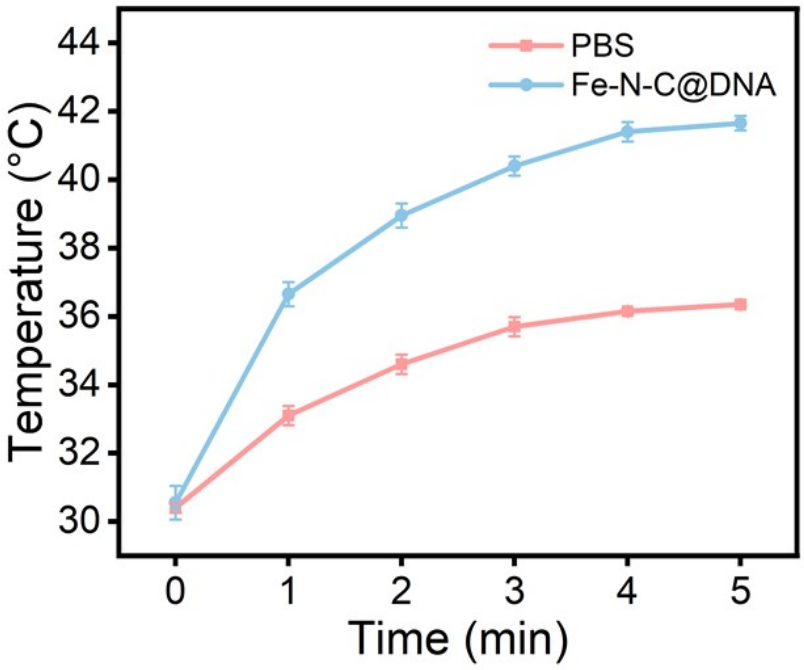

Fig. S28 Temperature change curves of MCF-7 tumor-bearing mice treated with saline, and Fe-N-C@DNA under 808 nm laser irradiation (0.5 W cm^{-2}).

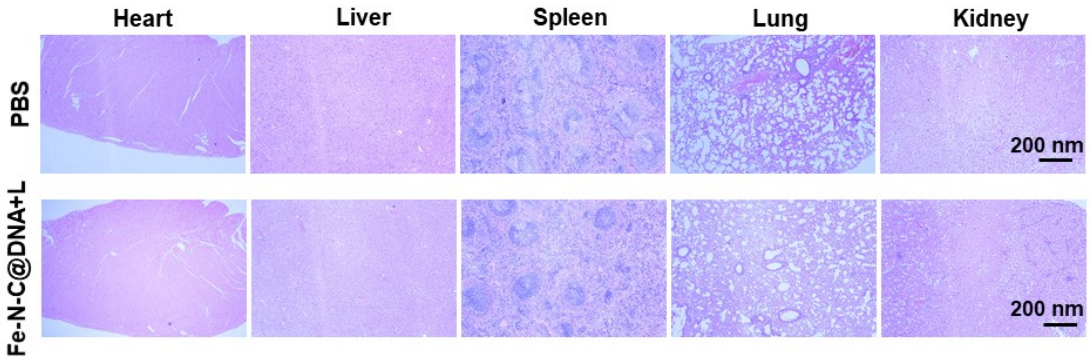

Fig. S29 H&E staining of the major organs after different treatments.

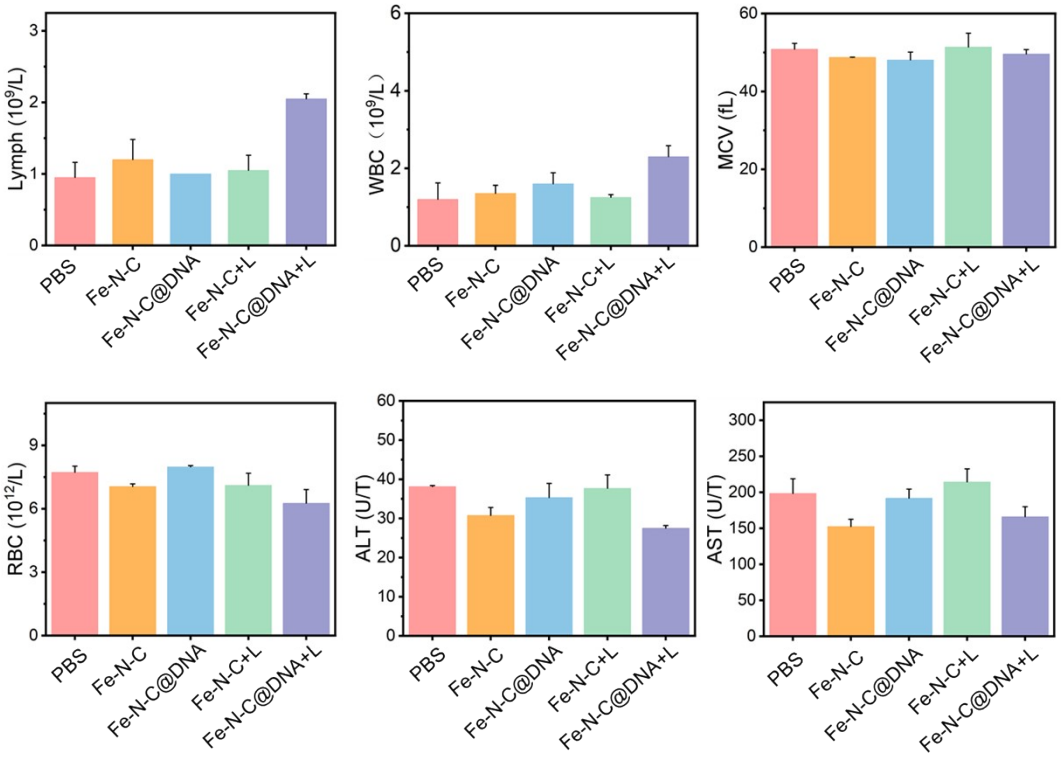

Fig. S30 Routine blood analysis and biochemical blood analysis of MCF-7-bearing mice 14 days after treatments. The terms include lymph, white blood cells (WBC), mean corpuscular volume (MCV), red blood cells (RBC), aspartate transaminase (AST), and alanine aminotransferase (ALT).

References

1 M. Huo, L. Wang, Y. Wang, Y. Chen and J. Shi, *ACS Nano*, 2019, **13**, 2643-2653.

2 M. Huo, L. Wang, H. Zhang, L. Zhang, Y. Chen and J. Shi, *Small*, 2019, **15**, 1901834.

3 S. Wang, Z. Hu, Q. Wei, P. Cui, H. Zhang, W. Tang, Y. Sun, H. Duan, Z. Dai, Q. Liu and X. Zheng, *ACS Appl. Mater. Interfaces*, 2022, **14**, 20669-20681.